Quantification of Lewis acid sites in 3D and 2D TS-1 zeolites: FTIR spectroscopic study

Mariya Shamzhy, Jan Přech, Jin Zhang, Valérie Ruaux, Hussein El-Siblani, Svetlana Mintova

Quantification of Lewis acid sites in 3D and 2D TS-1 zeolites: FTIR spectroscopic study

Mariya Shamzhy*,[1], Jan Přech[1,2], Jin Zhang[1], Valérie Ruaux[2], Hussein El-Siblani[2], Svetlana Mintova[2]

[1] *Department of Physical and Macromolecular Chemistry, Faculty of Science, Charles University, Hlavova 2030/8, 128 43 Prague 2, Czech Republic*

[2] *Normandie Université, ENSICAEN, UNICAEN, CNRS, Laboratoire Catalyse et Spectrochimie, 14000 Caen*

*Corresponding author: mariya.shamzhy@natur.cuni.cz

Keywords: TS-1, layered zeolites, acidity, FTIR, molar extinction coefficient

Abstract

Titanium silicalite 1 (TS-1) zeolite is an important selective oxidation catalyst. Recently prepared layered and pillared forms expanded the application of TS-1 to the catalytic oxidation of bulky molecules. Despite progress in designing and application of titanosilicate zeolites in catalysis, only qualitative information of their acidity is available. Herein, we report thorough characterization of acid sites in TS-1 zeolites of different morphologies (3D TS-1, layered 2D TS-1, 2D TS-1 pillared either with silica (TS-1-PISi) or silica-titania (TS-1-PITi)) using FTIR spectroscopy and probe molecules. FTIR of adsorbed pyridine was used for quantification of Ti-associated Lewis acid sites based on the integral intensity of υ_{8a} absorption band ca. 1608 cm^{-1} and measured integrated molar extinction coefficient (ε_{1608}(Ti-LAS) = 0.71± 0.01 cm μmol^{-1}). Thermodesorption of pyridine monitored with FTIR showed that distribution of strength of Lewis acid sites is, to some extent, dependent on the way of Ti incorporation in the samples. TS-1-PITi, containing large fraction of external surface Ti(OH)(OSi)$_3$ species introduced post-synthesis, showed increased concentration of stronger Lewis acid centres. FTIR spectroscopy of TS-1 with pre-adsorbed quinoline and d$_3$-acetonitrile probe confirmed enhanced relative concentration of external Lewis acid sites in all layered TS-1 materials (28–38%) vs. 3D TS-1 (2 %).

1. Introduction

Titanosilicate zeolites are well established selective oxidation catalysts with the ability to activate aqueous hydrogen peroxide. Titanosilicate zeolites, particularly titanium silicalite 1 (TS-1, **MFI** topology [1, 2]) are used industrially in propylene epoxidation, phenol hydroxylation, and cyclohexanone ammoxidation [3, 4]. In addition, they catalyse epoxidation of C=C double bonds in general (e.g. in linear and cyclic olefins or terpenes), oxidation of alkanes to corresponding alcohols, oxidation of alcohols to ketones and organic sulfides to sulfoxides and sulfones [5, 6].

Titanosilicate zeolites have titanium atoms isomorphously incorporated in the framework. These four-coordinated Ti atoms act like weak Lewis acid sites, coordinating hydrogen peroxide. Until today, about 17 type zeolites have been prepared in the titanosilicate form, either by direct hydrothermal synthesis or by post-synthesis modification. These include the TS-1 (MFI), Ti-beta (*BEA) [7], Ti-MWW [8], Ti-MOR [9], Ti-MSE [10], Ti-CON [11] and others. Also, various hierarchical and layered forms, particularly derived from TS-1, Ti-MWW [12] and Ti-UTL [13] were prepared. The main reason to develop the hierarchical and layered titanosilicates is to reduce diffusion limitations for sterically demanding substrates in conventional zeolites [14]. Sterically demanding substrates such as cyclic olefins and terpenes cannot access the narrow micropores of medium-pore zeolites (e.g. MFI d_p = 5.5 Å), and improvement provided by use of large-pore zeolite (e.g. Ti-beta) is not always sufficient.

Layered titanosilicates are obtained when a corresponding zeolite is formed *via* a layered precursor (e.g. Ti-MWW [8], Ti-FER [15]) or they can be prepared using the surfactant templated synthesis (layered TS-1 [16]) or using the ADOR protocol (Ti-UTL derived materials [13]). Properties of layered titanosilicates can be tuned by post-synthesis transformations, particularly by varying the interlayer distance and/or introducing new species between the layers [17]. One of such transformations is pillaring of a swollen layered titanosilicate (in a swollen material, the interlayer distance is expanded by introducing a surfactant in between the layers).

In a pillared material the layers are supported by amorphous silica pillars and thus they do not collapse upon calcination [12]. Recently, we have demonstrated that by introducing additional titanium source at pillaring step, highly active catalysts for epoxidation of cyclic olefins and terpenes are formed [13, 18].

Comparing the catalysis data in literature [19] and our experimental results [13, 18, 20], it can be observed that the decrease in diffusion limitations improves the catalytic activity of nanosheet vs. conventional 3D titanosilicate zeolites. However, despite a big progress in designing and applying titanosilicate zeolites in catalysis, only qualitative information on the acidity is available mainly for 3D TS-1. The results of UV-Vis, FTIR and XANES spectroscopies of adsorbed probe molecules have revealed the presence of coordinatively unsaturated Ti-sites acting as Lewis acid centres in TS-1 [21-24]. In particular, Bonino et al. reported evidence for the Lewis acid character of the tetrahedral Ti sites in TS-1 based on the FTIR spectroscopy using adsorbed d_3-acetonitrile and pyridine as complementary probe molecules. FTIR spectra of pyridine adsorbed on dehydrated TS-1 [21, 22], Ti-beta [21] and Ti-MWW [25] zeolites have also indicated the presence of only Lewis acid sites. Although the nature of acid centers was unambiguously addressed for different 3D titanisolicate zeolites, to the best of our knowledge, (i) quantification of Lewis acid sites as well as (ii) estimation of acid sites distribution with respect to their strength, both influencing the catalytic behaviour of titanosilicate zeolites, have not been explored so far either for 3D or 2D TS-1 catalysts.

Besides providing valuable qualitative information on the surface chemical properties of zeolites, FTIR spectroscopy is also a powerful tool for quantitative characterization of the nature, strength and location of their active sites [26, 27].

D_3-acetonitrile (proton affinity (PA) = 783 kJ/mol), pyridine (PA = 912 kJ/mol) and alkyl-pyridines are the most frequently used molecules to probe the acidity of aluminosilicates [27]. The FTIR spectroscopy of adsorbed pyridine is usually applied for identifying the nature and quantifying the amount of acid sites in medium- and large-pore zeolites using absorption bands characteristic of pyridine adsorbed on Al-associated Brønsted (1545 cm^{-1}) and Lewis acid centres (~1450 cm^{-1}) [28, 29]. Temperature-programmed desorption of pyridine [30, 31] and alkylpyridines are widely used to assess the strength of acid sites located either in zeolite micropores or on the external surface.

In contrast, ammonia and d_3-acetonitrile- are more suitable probe molecules for the quantitative analysis of acid centres in small-pore zeolites, while substituted nitriles (e.g., propionitrile, 2,2-dimethylpropionitrile, isobutyronitrile and others) have been used for the quantification the accessibility of acid sites in zeolites [32-35].

Being well established particularly for aluminosilicate catalysts, FTIR spectroscopy has been so far undeservedly underused for titanosilicates.

Herein, we report the results of detailed characterization of acid sites in titanosilicate MFI zeolites of different structures and morphologies (3D TS-1, lamellar 2D TS-1, 2D TS-1 pillared either with silica TS-1-PISi or silica-titania TS-1-PITi) using FTIR spectroscopy of adsorbed probe molecules. FTIR of adsorbed pyridine (kinetic diameter of 5.4 Å) characterized by relatively high basic strength was used for quantification of Ti-associated Lewis acid sites. For that, we used υ_{8a} absorption band ca 1608 cm^{-1} and determined corresponding molar extinction coefficient. The quantification of weak Lewis acid sites in TS-1 zeolites using υ_{19b} absorption band ca 1445 cm^{-1} was impeded by unavoidable contribution of H-bonded pyridine to the intensity of υ_{19b}.band. A combination of pyridine-FTIR with thermal desorption provided an estimate of the acid strength distribution in titanosilicate zeolites under the study. Moreover, an accessibility of Lewis acid sites in 3D and 2D TS-1 catalysts was addressed by selective poisoning of external sites with quinoline (QUI, kinetic diameter 6.2 Å) and subsequent quantification of the internal sites using FTIR of adsorbed d$_3$-acetonitrile (ACN, kinetic diameter 4.0 Å).

2. Experimental

2.1 Catalysts preparation

3D TS-1(a) catalyst was a commercial TS-1 provided by Zeolyst International. 3D TS-1(b) catalyst was synthesized from a gel with an initial molar composition 100 TEOS : 2.32 Ti(OBu)$_4$: 35 TPA-OH : 4000 H$_2$O following a procedure form ref [36]. TEOS stands for tetraethyl orthosilicate; Ti(OBu)$_4$ stands for titanium(IV) butoxide; TPA-OH stands for tetrapropylammonium hydroxide which acted as a structure directing agent.

2D TS-1 was prepared following a restricted crystal growth protocol developed by Na et al. [16] and more specifically following the protocol reported in ref. [18]. In short: a bromide-free surfactant template C$_{18}$H$_{37}$N$^+$(CH$_3$)$_2$-C$_6$H$_{12}$N$^+$(CH$_3$)$_2$-C$_6$H$_{13}$ in a hydroxide form (C$_{18-6-6}$OH$_2$) was used for the preparation of a synthesis mixture with a molar composition 100 TEOS : 2.5 Ti(OBu)$_4$: 6 C$_{18-6-6}$OH$_2$: 5000 H$_2$O. The zeolite was hydrothermally synthesized in a Teflon-

lined autoclave at 155°C for 236 h under agitation. Final product was collected by filtration, washed with distilled water, dried and part of it was calcined at 550°C for 8 h with a temperature ramp of 2°C. The remaining part was divided into two and was subjected to silica (yielding TS-1-PISi) or silica-titania pillaring (yielding TS-1-PITi).

Both TS-1-PISi and TS-1-PITi were prepared following the procedures reported by our group earlier [18]. In short, the as-synthesized 2D TS-1 was pillared using a TEOS (20 ml/g of zeolite) in case of TS-1-PISi and using a mixture of TEOS and TBOTi in mass ratio 30:1 in case of TS-1-PITi. The zeolite was mixed with the pillaring medium and stirred at 65°C for 24 h. After the given time, the product was centrifuged, dried, hydrolyzed in water with 5% of ethanol for another 48 h and finally filtered, dried and calcined at 550°C for 8 h with a temperature ramp of 2°C.

2.2 Catalysts basic characterization

The structure and crystallinity of all materials was determined by X-ray powder diffraction using a Bruker AXS D8 Advance diffractometer equipped with a graphite monochromator and a position-sensitive detector Våntec-1 using Cu Kα1 radiation (45 kV and 40 mA) in Bragg–Brentano geometry. The X-ray scanning was performed in continuous scan mode in the range of 1 - 40° (2θ).

The size and shape of zeolite crystals were examined by scanning electron microscopy (SEM) on a JEOL, JSM-5500LV microscope or a MIRA TESCAN microscope. The images were collected with an acceleration voltage of 30 kV. Samples were platinum sputtered before measurement.

The BET area and pore volume of all catalysts were determined by nitrogen physisorption at -196 °C using a 3Flex (Micromeritics) static volumetric apparatus. The degassing of the samples was performed prior to the measurement in a stream of helium at 300°C for 3 h. The surface area was calculated using BET method in the range of relative pressures $p/p_0 = 0.05$-0.20 [37]. The adsorbed amount of nitrogen at $p/p_0 = 0.95$ reflects the total pore volume. The volume of micropores and the external surface area were determined using *t*-plot method [38].

Chemical composition of the materials (expressed as a Si/Ti ratio) was determined by Thermo Scientific iCAP-7600 inductively coupled plasma optical emission spectrometer (ICP-OES) equipped with peristaltic pump with a drain sensor, free-running 27.12 MHz solid state RF plasma generator, charge injection device detector (CID86) with the range of 166 – 847 nm and

CETAC ASX 520 auto sampler. 50 mg of zeolite was mineralized in a mixture of 1.8 ml of 48 % HF, 1.8 ml of 67 % HNO_3, and 5.4 ml of 36 % HCl in the microwave oven. After cooling, the HF excess was eliminated by the complexation with 13.5 ml of saturated solution of H_3BO_3 and final mixture was treated in microwave oven again. Thereafter, the solution under analysis was collected and diluted by ultrapure water to a total volume of 250 ml.

Diffuse reflectance ultraviolet-visible (DR-UV/Vis) spectra were collected using Perkin-Elmer Lambda 950 Spectrometer. For that, a 2 mm quartz tube was filled with the sample. The spectra were collected in a wavelength range of 190-500 nm and converted to absorption spectra using the Kubelka-Munk function.

^{29}Si-MAS-NMR spectra were collected on a Bruker Avance III HD 500 MHz spectrometer. Chemical shifts were referred to tetramethylsilane. All samples were measured in calcined state using a sample spinning speed of 18 kHz.

2.3 Characterization of acid centres using FTIR of adsorbed probe molecules

2.3.1 Nature and concentration of acid sites

The concentration of Lewis acid sites (LAS) in titanosilicate zeolites was determined by pyridine-FTIR based on the intensities of characteristic absorption band (a.b.) at 1608 cm^{-1}. The zeolites were pressed into self-supporting wafers with a density of ~10 mg/cm^2 and *in situ* activated at T = 450 °C and p = 5·10^{-5} Torr for 4 h.

To determine the temperature of PY adsorption/desorption sufficient for removal of H-bonded probe molecule while maintaining PY coordinatively-bonded to Ti-associated Lewis acid sites, an excess of PY (cca. 2 mmol PY per 1 g of zeolite) was adsorbed at 25°C, 50°C, 80°C, 100°C, 120°C, 150°C and 200°C in 3D TS-1(a) sample. For each temperature 10-minute adsorption and 10-minute desorption took place. FTIR spectra were recorded using a Nicolet iS50 spectrometer with a transmission MTC/B detector with a resolution of 4 cm^{-1} by collecting 128 scans for a single spectrum at room temperature. The spectra were treated using Omnic 8.2 (Thermo Scientific) program. For the baseline correction, spectrum of activated wafer was subtracted from the spectra collected after pyridine adsorption/desorption. To determine the area of the peaks characteristic for coordinatively bonded (1608 cm^{-1}) and H-bonded (1596 cm^{-1}) pyridine the

6

resultant spectral curve was fitted using Gaussian line shape. IR peak centers were fixed within ± 5 cm^{-1}, and the full widths at half maxima were constrained to be between 5 cm^{-1} and 20 cm^{-1}. For quantification of the concentrations of LAS in TS-1(a) samples, PY adsorption was carried out at 50°C (found to be optimal for the quantitative study of titanosilicates) and a partial pressure of 3.5 torr for 10 min followed by desorption for 10 min at the same temperature. C(LAS) were evaluated from the integral intensities of a.b. at 1608 cm^{-1} using molar absorption coefficients ε_{1608}(Ti-LAS) = 0.71±0.01 cm µmol^{-1} determined from the linear relationship between [integrated IR band area (cm^{-1})*wafer cross sectional area (cm^2)] and the total moles dosed (µmol) similar to Ref. [39-41].

2.3.2. Strength of acid sites

Thermodesorption of PY was carried out at 50, 100, 150 and 200 °C for 10 min. Distribution of Ti-associated acid centers with respect to their strength was analyzed based on the relative concentration of acid sites bearing pyridine molecules at elevated temperatures:

$$I_{1608} (T°C) / I_{1608} (50°C) \qquad\qquad (Eq.\ 1)$$

where

I_{1608} (X°C) refers to the intensity of a.b. at 1608 cm^{-1} in the FTIR spectra of titanosilicate zeolites after activation followed by pyridine adsorption/desorption at T = X°C (X is 100, 150 and 200 °C).

2.3.3. Accessibility of acid sites

The ratio between "internal" acid sites and those located on the external surface of zeolite crystals ("external" acid centers) of TS-1 catalysts was evaluated based on the analysis of FTIR spectra of ACN adsorbed in the catalysts either after activation or after pre-adsorption of bulky QUI selectively poisoning "external" acid sites as discussed in Ref. [42, 43]. ACN adsorption was performed according to the Ref. [44], while pre-adsorption of QUI was carried out according to the protocol described in Ref. [45]. The concentrations of Ti-LAS were semi-quantitatively estimated from the integral intensities of a.b. at 2304 cm^{-1}. The fraction of „external" acid sites was evaluated as

$$[I_{2304} (ACN)-I_{2304} (QUI+ACN)]/ I_{2304} (ACN) \qquad\qquad (Eq.\ 2)$$

where

I_{2304} (ACN) refers to the intensity of a.b. at 2304 cm^{-1} in the FTIR spectra of titanosilicate zeolites after activation followed by ACN adsorption;

I_{2304} (QUI+ACN) refers to the intensity of a.b. at 2304 cm^{-1} in the FTIR spectra of titanosilicate zeolites after activation followed by co-adsorption of quinoline and ACN.

2.4 Characterization of acid centres using TPD of ammonia

Ammonia temperature programmed desorption (TPDA) was measured using the AutoChem II 2920 (Micromeritics, USA). Typically, 100 mg of of zeolite (with grain size 0.25–0.5 mm) was inserted into quartz tubular reactor and anchored by quartz wool. Prior to TPD experiment, sample was heated in helium flow of 25 mL min^{-1} from room to the 250 °C with defined heating rate of 10 °C min^{-1} and held at final temperature for 10 min. Then the sample was cooled down to the 50 °C in the flow of helium (25 mL min^{-1}). Saturation of sample with ammonia was carried out by flowing the sample bed by gas mixture of helium and ammonia (5 vol% of ammonia in He) with flow rate 10 mL min^{-1} at 50 °C for 30 min followed by removing of weakly bounded molecules by flushing sample out under flow of helium (25 mL min^{-1}) for 30 min. Finally, TPD experiment was carried out by increasing temperature from 50 to 400 °C, at which sample was held for 5 min. The desorbed ammonia in the outlet gas was detected using thermal conductivity detector (TCD) and mass spectrometer (MS) Pfeiffer OmniStar GSD 300, Balzers, on which the mass m/e = 4 (He$^+$), 15 (NH$^+$), 16 (NH$_2^+$), 17 (NH$_3^+$), and 18 (H$_2$O$^+$) was monitored.

3. Results and discussion

3.1 Catalyst characterization

XRD patterns of studied catalysts (Supplementary Information (SI), Fig. S1) confirm that all of the titanosilicates synthesized have the structure intended to be obtained. Three well-defined peaks at 7.9°, 8.8°, and 8.9° 2θ corresponding to (011), (020) and (200) reflections are visible in the pattern of 3D TS-1 zeolite evidencing well-ordered structure with typical MFI architecture. In contrast, absence of the (hkl) reflections with k≠0 in the XRD patterns of both lamellar 2D TS-1 and pillared TS-1-PI catalysts indicate that the thickness of zeolite crystallites is extremely low in (010) direction (along the crystallographic b-axis). Successful pillaring of the TS-1-PITi

and TS-1-PISi is proven by the presence of intensive low angle peak at 1.5° 2θ, which is characteristic of the preservation of the interlayer distance originally present in the as-synthesized 2D TS-1. This diffraction peak is not present in the XRD pattern of calcined 2D TS-1. Both 3D TS-1(a) and 3D TS-1(b) show N_2 adsorption isotherms of I type characteristic of purely microporous materials, while 2D TS-1, TS-1-PITi and TS-1-PISi were characterized by non-reversible isotherms of type II with H3 hysteresis which is typically observed for non-rigid aggregates of plate-like particles giving rise to slit-shaped mesopores. (Fig. S2) [46].

The SEM images of 3D TS-1 (a) (SI, Fig. S3a) and 3D TS-1 (b) (SI, Fig. S3b) show that the samples are composed of crystals with a size of 200 nm and 600 nm, respectively. In contrast, 2D TS-1 (SI, Fig. S3c), TS-1-PITi (SI, Fig. S3d) and TS-1-PISi (SI, Fig. S3e) are composed of aggregated nanosheet crystals.

Titanium content, crystal size and textural properties of the TS-1 catalysts are summarized in Table 1. Note the differences in Si/Ti ratio between 2D TS-1 (Si/Ti=44), TS-1-PISi (Si/Ti=55) and TS-1-PITi (Si/Ti=19) are caused by dilution of the parent 2D TS-1 with silica pillars in TS-1-PISi and formation of additional titanium sites in TS-1-PITi, respectively [18].

UV/Vis spectra of the studied catalysts are presented in Figure 1. The spectra of both 3D TS-1 samples and 2D TS-1 contain only one absorption band centred at 205 nm, which is characteristic of framework tetrahedrally coordinated titanium species [24]. The TS-1-PISi contains an additional band at approx. 260 nm, characteristic of isolated 5-coordinated titanium species [24]. The TS-1-PITi contains the same band with higher intensity. Presence of 5-coordinated Ti species may have two reasons. In the TS-1-PITi, majority of the 5-coordinated extra-framework species is formed in the silica-titania pillaring step, when the additional Ti source reacts with the surface of the crystalline layers. In contrast, the origin of 5-coordinated species in TS-1-PISi is not so clear. It is unlikely that Ti atoms were extracted from framework positions during pillaring or calcination; however, the observed band may represent originally surface framework Ti atoms now in contact with the amorphous silica pillars.

Table 1: Chemical composition and textural properties of 3D and 2D TS-1 catalysts

Zeolite	Si/Ti*	Crystal size*	BET m^2/g	S_{ext} m^2/g	V_{mic} cm^3/g	V_{tot} cm^3/g
3D TS-1(a)	28	200 nm	510	63	0.10	0.28

3D TS-1(b)	39	600 nm	450	60	0.13	0.22
2D TS-1	44	nanosheets	576	318	0.12	0.63
TS-1-PITi	19	nanosheets	591	338	0.10	0.55
TS-1-PISi	55	nanosheets	575	180	0.11	0.39

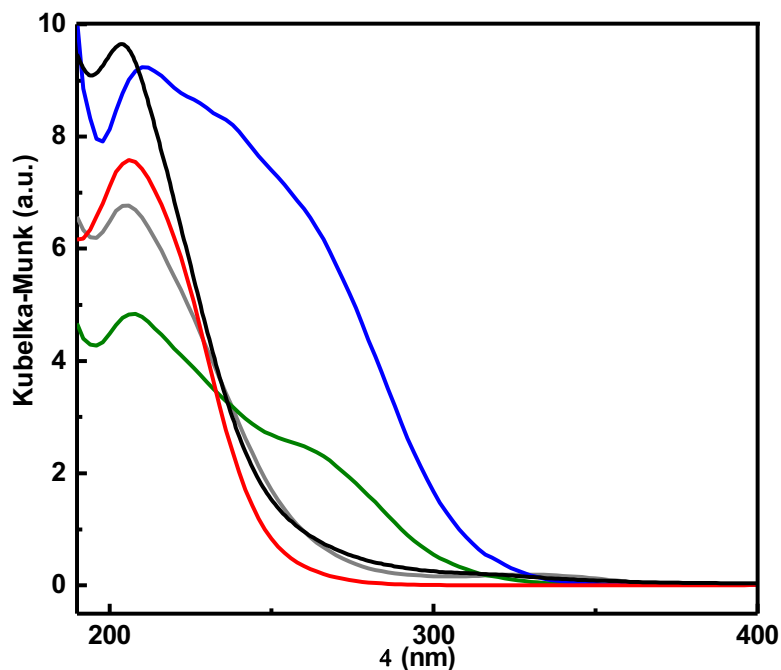* Titanium content was determined by ICP-OES analysis; crystal size was determined by SEM

Figure 1. DR-UV/Vis spectra of 3D TS-1(a) (gray), 3D TS-1(b) (black), 2D TS-1 (red), TS-1-PISi (green), and TS-1-PITi (blue)

Remarkable increase in external surface area for 2D forms of the TS-1 (180-340 m^2 g^{-1}, Table 1) vs. 3D TS-1(60 m^2 g^{-1}, Table 1) was accompanied with increasing number of silanol defects, as detected by ^{29}Si MAS NMR. The Q^3 Si species at -102 ppm and Q^4 Si species at -114 ppm were observed for all titanosilicates under the study (Fig. 2). Selective enhancement of the resonance band at -102 ppm in the ^1H-^{29}Si cross polarization (CP) MAS NMR experiment (Fig. 2) evidenced the assignment of respective signal to silicon atoms that are coupled with the hydrogens of the hydroxyl groups by dipolar interaction, i.e., to $(SiO)_3$**Si**-OH moieties.
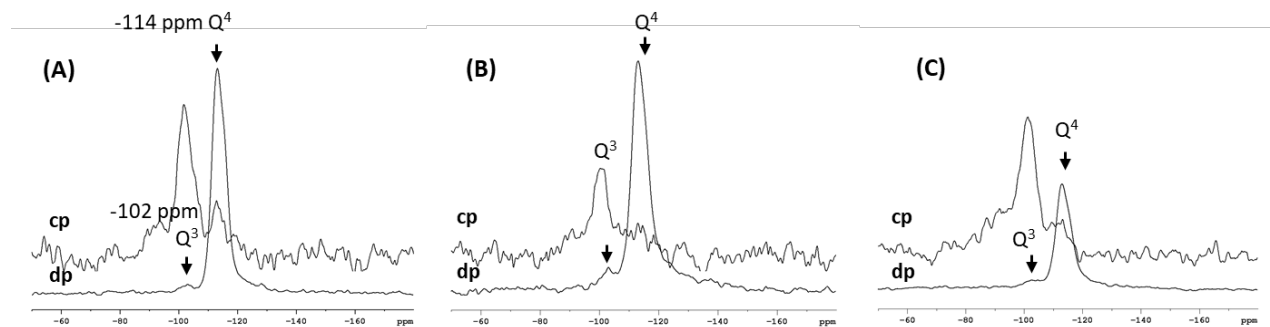
Figure 2. Direct pulse ^{29}Si MAS NMR (dp) and ^{1}H-^{29}Si CP/MAS NMR (cp) spectra of titanosilicates (A) TS-1(b), (B) 2D TS-1 and (C) TS-1-PITi

Thus, according to their basic characteristics, the prepared titanosilicates are qualified as representative 3D- and 2D TS-1 zeolites, being appropriate for comparative study on the number, strength and accessibility of Ti-associated acid sites.

3.2 Acidity of TS-1 catalysts

3.2.1 Nature, concentration and strength of acid sites

Pyridine, a versatile base molecule for probing zeolite acidity [26], was used for qualitative and quantitative study of acid sites in TS-1 catalysts in this work. The FTIR spectra of the activated TS-1 zeolites displaying the characteristic bands of free silanol groups (3743 cm^{-1}) are shown in Fig. 3 (A). Higher intensity of respective band is typical for all 2D catalysts, which is consistent with the higher external surface area of layered zeolites (Table 1) and thus increased content of terminal silanol groups. The adsorption of an excess of pyridine, followed by evacuating of physically adsorbed probe molecules gave rise to new absorption bands in 1700-1400 cm^{-1} region (Fig. 3B). While the υ_{8b} (1577 cm^{-1}), υ_{19a} (1490 cm^{-1}) and υ_{19b} (1445 cm$^{-1)}$ a.b. of H-bonded and LAS-Py convolutes, the υ_{8a} a.b. are well-distinguishable at 1596 cm^{-1} (υ_{8a}-H) and 1608 cm^{-1} (υ_{8a}-LAS), respectively [26, 47]. On the other hand, no υ_{19b} absorption band characteristic of Brønsted acid sites (1545 cm^{-1}) was detected for materials under investigation, which is in line with previous reports [48, 49] as well as with character of the materials (containing no T^{3+} atoms).
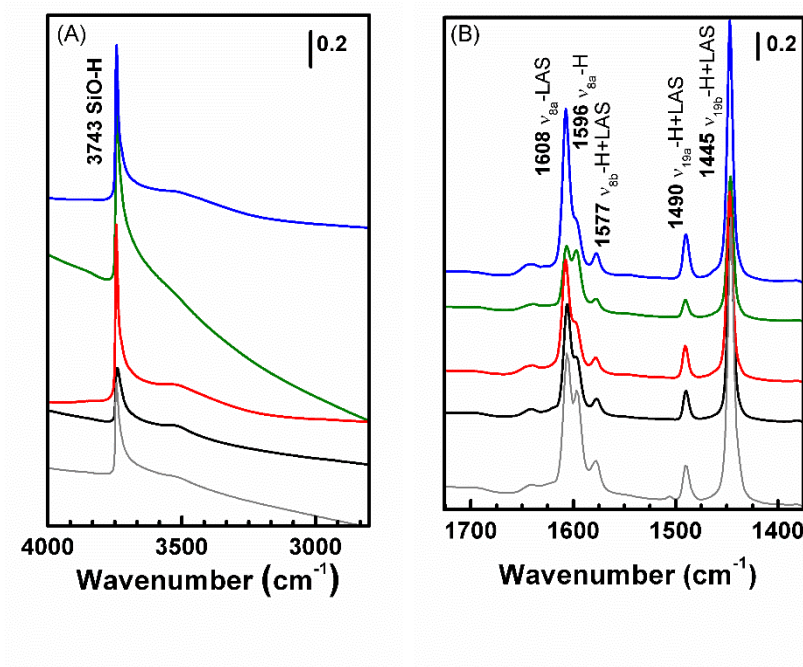
Figure 3. FTIR spectra of 3D TS-1(a) (gray), 3D TS-1(b) (black), 2D TS-1 (red), TS-1-PISi (green), TS-1-PITi (blue) activated zeolites (A); spectra after adsorption/desorption of an excess of pyridine at 50 °C (B)

Relative intensities of respective ν_{8a} bands were found dependent on the temperature of pyridine adsorption/desorption (the spectra of 3D TS-1(a) zeolite are shown as representative in Fig. 4A). Intensity of ν_{8a}-LAS band at 1608 cm⁻is almost constant at T = 25 – 50 °C. At the same time, 20 – 25 % decrease of either ν_{8a}-H or ν_{19b}-H+LAS band intensity was observed at T = 50 °C vs. T = 25°C (Fig. 4B). Further increase in adsorption/desorption temperature resulted not only in removal of the most of H-bonded pyridine (54-96% decreasing ν_{8a}-H at T= 70 – 150 °C), but also substantially reduced the intensity of ν_{8a}-LAS band (25-73% decreasing ν_{8a}-LAS at T= 70 – 150 °C). Difference spectra obtained by subtraction of the spectrum of activated zeolite from the ones after adsorption/desorption of pyridine show the region of OH vibrations (Fig. 4B). Decrease in intensity of absorption band ca 3743 cm⁻¹ with increasing adsorption/desorption temperature is indicative for reducing contribution of H-bonded pyridine.
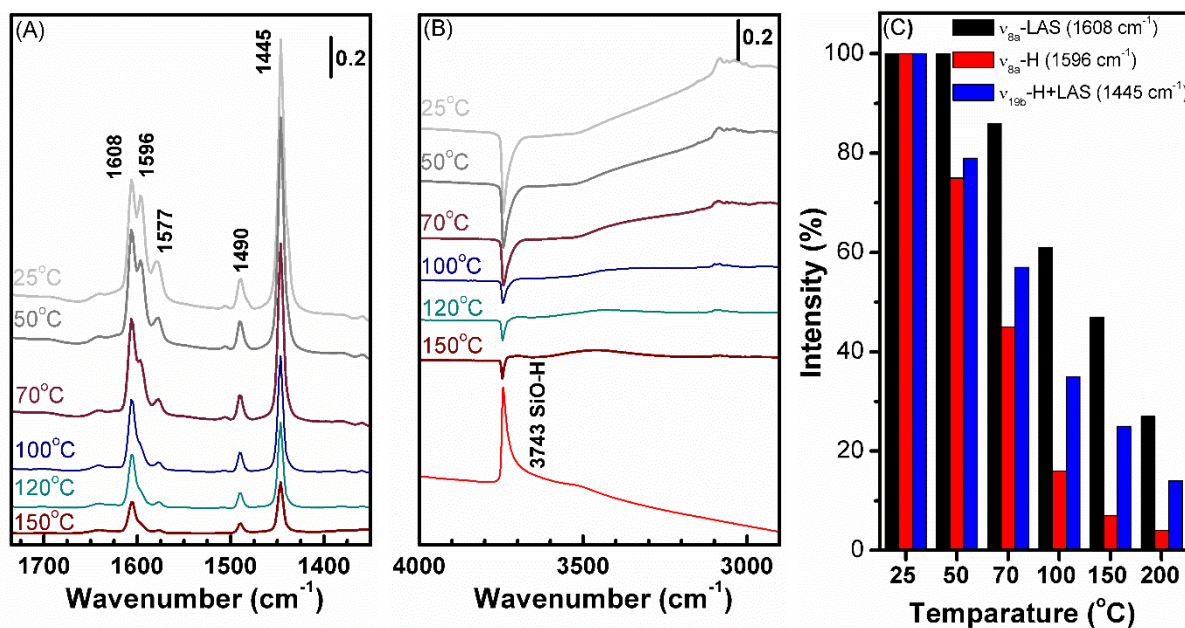
12

Figure 4. FTIR spectra of 3D TS-1(a) after adsorption/desorption of pyridine at different temperatures in the region of pyridine vibrations (A). Difference FTIR spectra after adsorption/desorption of pyridine at different temperatures are compared with the spectrum of activated 3D TS-1(a) zeolite (–) in the region of OH vibrations (B). Relative change of the intensities of a.b. at 1596 cm^{-1} (υ_{8a}-H) and 1608 cm^{-1} (υ_{8a}-LAS) vs. temperature of pyridine adsorption/desorption in 3D TS-1 zeolite (C).

Thus, low strength of Ti-associated LAS precludes full removal of H-bonded pyridine while maintaining coordinatively bonded probe molecules and therefore impedes use of routine FT-IR acidity analysis protocol widely applied for aluminosilicate zeolites (i.e., (i) saturation of the sample with pyridine at T = 150 – 200 °C; (ii) evacuating the sample at the same temperature and (iii) monitoring the intensity of υ_{19b} 1445 cm^{-1} band [26]). In contrast, using the intensity of υ_{8a}-LAS was found sufficient for quantification of LAS in TS-1 catalysts after adsorption of pyridine at 50 °C. Adsorbing pyridine, the first small doses gave rise only to υ_{8a}-LAS, while υ_{8a}-H started to increase only after adding certain amount of the probe molecules. Thus, special attention was paid to proper choice of the range of pyridine concentrations (e.g., <1.2 μmol/cm^2, Fig. 5) enabling to neglect contribution of H-bonded pyridine to the value of molar absorption coefficient ε$_{1608}$(Ti-LAS). Indeed, careful analysis of the difference FTIR spectra collected in OH

13

vibration region at increasing dosing of adsorbed pyridine revealed negligible contribution of H-bonded probe molecule when the overall adsorbed amount did not exceed 1.2 μmol/cm^2 (Fig. 5B). Fig. 5 shows the results obtained by adsorbing increasing quantities of pyridine in 3D TS-1 at 50 °C. In our experiments, the intensity of υ_{8a}-LAS at 1608 cm^{-1} increases linearly with the amount of pyridine introduced. Thus, the extinction coefficient for the 1608 cm^{-1} band on 3D TS-1 zeolite was found to be equal to 0.71± 0.01 cm μmol^{-1}.
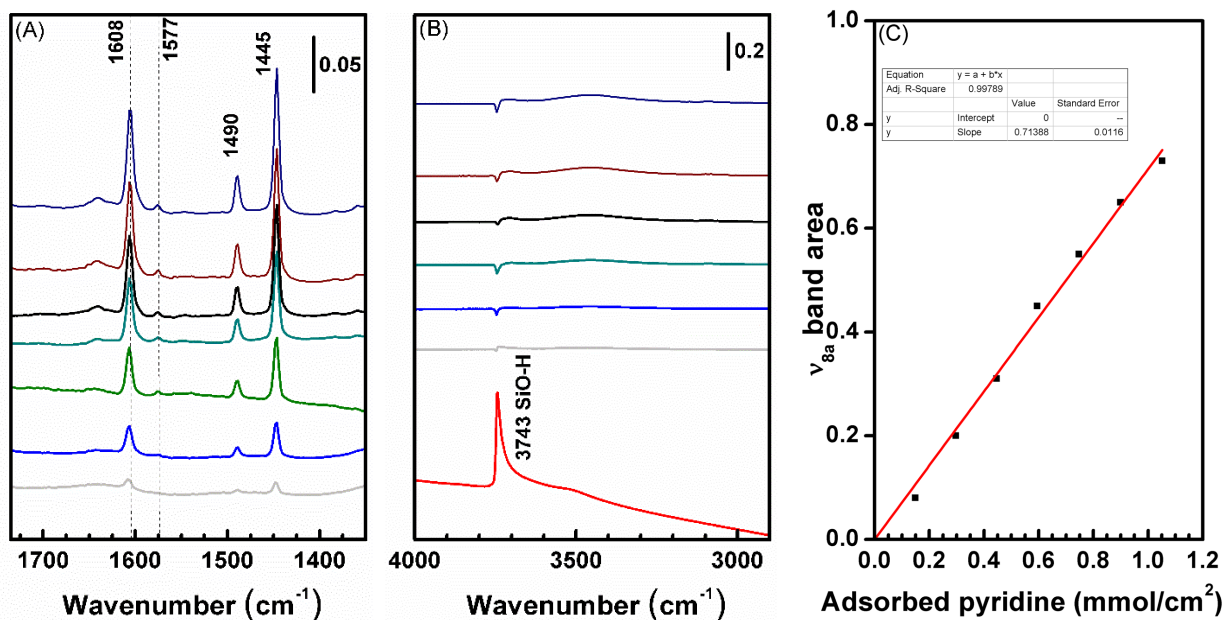

Figure 5. FTIR spectra of 3D TS-1(a) zeolite in the region of pyridine ring vibrations at increasing dosing of pyridine adsorbed at 50 °C (A). Difference FTIR spectra collected at increasing dosing of adsorbed pyridine are compared with the spectrum of activated 3D TS-1(a) zeolite (–) in the region of OH vibrations (B). Dependence of υ_{8a}-LAS (1608 cm^{-1}) band area on the concentration of adsorbed pyridine for 3D TS-1 (a) (C).

Once having the ε_{1608}(Ti-LAS) value, total concentration of Lewis acid sites was calculated based on the integral intensity of υ_{8a}-LAS (1608 cm^{-1}) after adsorption and consecutive desorption of an excess of pyridine at 50 °C. The total concentrations of Lewis acid sites in the TS-1 catalysts (Fig.3B) were found to decrease in the following order: TS-1-PITi (0.61 mmol/g) > 3D TS-1 (a) (0.55 mmol/g) > 3D TS-1 (b) (0.40 mmol/g) > 2D TS-1 (0.39 mmol/g) > TS-1-PISi (0.23 mmol/g). This is in agreement with the results of TPDA (Fig. S4) used as an independent method for verification the results of FTIR-Py for the chosen TS-1 zeolite samples

(Table 2). Indeed, TPDA using smaller ammonia probe molecule showed slightly higher values for the concentration of acid sites, but the difference with FTIR-Py results did not exceed 15 %. On the other hand, perfect consistence between the number of acid sites and chemical composition of 3D TS-1 zeolites containing mostly tetrahedral Ti atoms (Table 2) reveals unlimited accessibility of Lewis acid sites for pyridine molecules under experimental conditions used. In contrast to pyridine, recent reports state restricted conformational freedom of alkylated pyridines in the channels of MFI [50-52], which precludes the use of such bulky probe molecules for quantification of Lewis acid sites in zeolites with ≤10-ring channels. Instead, using of smaller molecular probes, e.g. ammonia, d_3-acetonitrile [26, 44] may give more complete results for small-pore zeolites. The difference between chemical composition and measured concentration of acid sites in the pillared samples (TS-1-PITi, TS-1-PISi) is observed most likely because a share of titanium is trapped inside or covered by the pillars and thus inaccessible.

Table 2: Concentration of Lewis acid sites in 3D and 2D TS-1 catalysts determined using FTIR-PY and TPDA

Sample	Chemical composition		Concentration of acid sites, mmol/g	
	Si/Ti	c(Ti) mmol/g	FTIR-Py	TPDA
3D TS-1(a)	28	0.57	0.55	0.56
3D TS-1(b)	39	0.41	0.40	0.47
2D TS-1	44	0.37	0.39	n.d.
TS-1-PITi	19	0.82	0.61	0.70
TS-1-PISi	55	0.30	0.23	n.d.

The distribution of Ti-associated LAS with respect to their strength was investigated by a stepwise thermodesorption of adsorbed pyridine while recording the residual intensity of the remaining characteristic υ_{8a}-LAS (1608 cm^{-1}) band. The part of LAS, which retained adsorbed pyridine at T = 150 – 200 ºC was evidently higher for TS-1-PITi, while all 3D TS-1 (a) and (b), 2D TS-1 and TS-1-PISi showed similar fraction of stronger LAS (Fig. 6). This result is most

likely connected with the contribution of Ti(OH)(OSi)$_3$ groups on the external surface of the titanosilicate layers created during the post-synthesis treatment. This result is in line with previous reports on the higher acid strength of mesostructured Ti-MCM-41 material and amorphous TiO$_2$–SiO$_2$ both bearing tripodal Ti(OH)(OSi)$_3$ moieties forming more stable Ti–pyridine complexes than the Ti(OSi)$_4$ sites in TS-1 [22, 24].

Figure 6. Fraction of LAS for TS-1 zeolites of different structures and morphologies vs. temperature of pyridine desorption

On the other hand, several FTIR studies reported on the strength of Brønsted acid sites [53, 54] and Lewis acid extra-framework Li$^+$ cations [55, 56] in 3D and 2D aluminosilicate zeolites. No significant differences in acidity strength between the 3D and 2D form of the same zeolite was found [54, 56] (e.g. MCM-22 vs. MCM-36 (pillared MWW layers) – a pair analogous to TS-1 and TS-1-PISi).

3.3.2 Accessibility of acid sites

To determine the amount of acid sites located on the external surface of TS-1 zeolite crystals, i.e., acid sites accessible for bulky substrates, we first adsorbed quinoline to poison the external acid sites and subsequently we introduced d$_3$-acetonitrile (ACN) to determine the internal acid centres. The strength of ACN bonding to acid sites is reflected in the shift of the stretching mode of ν(C≡N) to higher frequencies if to compare with 2265 cm^{-1} characteristic of ACN in liquid phase [57]. In particular, the spectra of ACN adsorbed in TS-1 zeolites (spectra of 2D TS-1

shown as an example in Fig. 7A) contain a single band at 2304 cm^{-1} attributed to CN vibration of the probe molecule interacting with weak Ti-associated Lewis sites as well as 2 other peaks corresponding to ACN adsorbed on silanol groups (2275 cm^{-1}), and physisorbed ACN (2265 cm^{-1}). IR spectra of ACN adsorbed on activated 2D TS-1 and those collected after QUI pre-adsorption are compared in Figure 7A. It can be seen that quinoline pre-adsorption obviously decreased the intensity of the peak I_{2304} attributed to the interaction between ACN and Ti-Lewis acid sites. Thus, the comparison between the I_{2304} (ACN) and I_{2304} (QUI+ACN) allow to determine the fraction of Ti-associated LAS located on the external surface of TS-1 crystals. Noticeably, all layered 2D TS-1, TS-1-PISi and TS-1-PITi zeolites showed similar fraction of external acid centers (28–38%, Fig.7B), while the fraction for 3D TS-1 was negligible (2 %, Fig.7B). These results are in agreement with previously reported higher catalytic activity of layered forms of TS-1 zeolites vs. 3D TS-1 in reactions involving bulky molecules [18, 19].
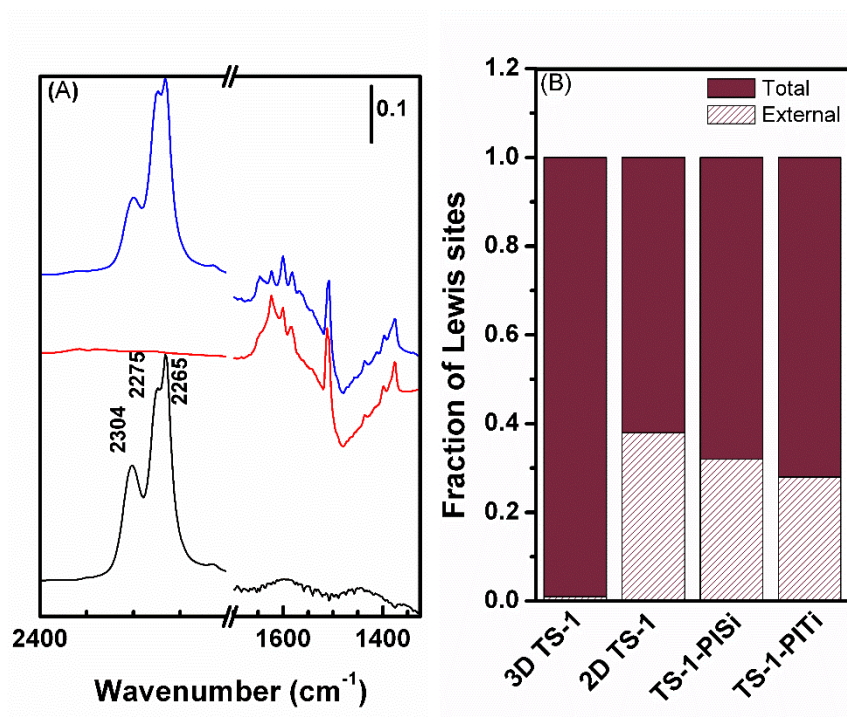

Figure 7. FTIR spectra of 2D TS-1 after adsorption of AN (black), quinoline (red), and co-adsorption of quinoline and d$_3$-acetonitrile (blue) (A). Fraction of external LAS in TS-1 catalysts determined using FTIR of co-adsorbed quinoline and d$_3$-acetonitrile (B)

4. Conclusions

Methodology for quantification of Lewis acid sites in titanosilicate zeolites using FT-IR analysis of adsorbed pyridine species was developed and applied to characterize TS-1 catalysts of different structures and morphologies (3D TS-1, lamellar 2D TS-1, 2D TS-1 pillared either with silica TS-1-PISi or silica-titania TS-1-PITi). The Ti-associated Lewis acid centres are, in contrast to aluminosilicate zeolites, of a low strength and this was found precluding the use of routine protocol to quantify LAS (i.e., monitoring the intensity of υ_{19b} 1445 cm^{-1} band [26]). Instead, the total concentration of Lewis acid sites in TS-1 catalysts was shown to be accurately determined after adsorption/desorption of an excess of pyridine at 50 °C from the integral intensity of υ_{8a}-LAS (1608 cm^{-1}) absorption band. Molar extinction coefficient for the respective band was determined ε_{1608}(Ti-LAS) = 0.71± 0.01 cm µmol^{-1}. Note this band can be used for quantification thank to absence of Brønsted acid sites in the titanosilicate zeolites.

Thermodesorption of pyridine monitored with FT-IR evidenced similar strength distribution of Lewis acid sites in all samples containing titanium introduced by direct hydrothermal synthesis (i.e. 3D TS-1, 2D TS-1 and TS-1-PISi). In contrast, the TS-1-PITi, containing share of titanium introduced by post-synthesis treatment (and previously shown to be the most active catalyst in cycloalkene-to-epoxide transformation [18, 19]), possessed increased concentration of strong Lewis acid centres.

FTIR spectroscopy of samples with pre-adsorbed quinoline and d$_3$-acetonitrile probe molecule confirmed the enhanced relative concentration of external Lewis acid sites in the layered TS-1 materials (28–38%) vs. 3D TS-1 (2 %). The results presented in this paper provide fundamental knowledge on the features of acid sites in the recently designed layered and pillared TS-1 zeolites, which will contribute to the development of heterogeneous selective oxidation catalysts.

References

[1] M. Taramasso, G. Perego, B. Notari, *Preparation of porous crystalline synthetic material comprised of silicon and titanium oxides* US 4410501

[2] R. Millini, E. Previde Massara, G. Perego, G. Bellussi, J. Catal. 137 (1992) 497-503.

[3] X. Lu, W.-J. Zhou, H. Wu, A. Liebens, P. Wu, Appl. Catal. A 515 (2016) 51-59.

[4] C. Perego, A. Carati, P. Ingallina, M.A. Mantegazza, G. Bellussi, Appl. Catal. A 221 (2001) 63-72.

[5] A. Korzeniowska, J. Grzybek, W.J. Roth, A. Kowalczyk, P. Michorczyk, J. Cejka, J. Prech, B. Gil, ChemCatChem 11 (2019) 520-527.

[6] M. Mazur, V. Kasneryk, J. Prech, F. Brivio, C. Ochoa-Hernandez, A. Mayoral, M. Kubu, J. Cejka, Inorg. Chem. Front. 5 (2018) 2746-2755.

[7] M.A. Camblor, A. Corma, A. Martinez, J. Perez-Pariente, J. Chem. Soc., Chem. Commun. (1992) 589-590.

[8] P. Wu, T. Tatsumi, T. Komatsu, T. Yashima, J. Phys. Chem. B 105 (2001) 2897-2905.

[9] P. Wu, T. Komatsu, T. Yashima, J. Phys. Chem. 100 (1996) 10316-10322.

[10] Y. Kubota, Y. Koyama, T. Yamada, S. Inagaki, T. Tatsumi, Chem. Commun. (Cambridge, U. K.) (2008) 6224-6226.

[11] J. Přech, D. Vitvarová, L. Lupínková, M. Kubů, J. Čejka, Microporous Mesoporous Mater. 212 (2015) 28-34.

[12] S.-Y. Kim, H.-J. Ban, W.-S. Ahn, Catal. Lett. 113 (2007) 160-164.

[13] J. Přech, J. Čejka, Catal. Today 277 (2016) 2-8.

[14] J. Prech, P. Pizarro, D.P. Serrano, J. Cejka, Chem Soc Rev 47 (2018) 8263-8306.

[15] A. Corma, U. Diaz, M.E. Domine, V. Fornes, Chem. Commun. (Cambridge, U. K.) (2000) 137-138.

[16] K. Na, C. Jo, J. Kun, W.S. Ahn, R. Ryoo, ACS Catal. 1 (2011) 901-907.

[17] W.J. Roth, P. Nachtigall, R.E. Morris, J. Čejka, Chem. Rev. 114 (2014) 4807-4837.

[18] J. Přech, P. Eliášová, D. Aldhayan, M. Kubů, Catal. Today 243 (2015) 134-140.

[19] J. Přech, Catal. Rev. 60 (2018) 71-131.

[20] J. Přech, M. Kubů, J. Čejka, Catal. Today 227 (2014) 80-86.

[21] D. Trong On, S.V. Nguyen, V. Hulea, E. Dumitriu, S. Kaliaguine, Microporous Mesoporous Mater. 57 (2003) 169-180.

[22] D. Srinivas, R. Srivastava, P. Ratnasamy, Catal. Today 96 (2004) 127-133.

[23] L. Wu, S. Zhao, L. Lin, X. Fang, Y. Liu, M. He, J. Catal. 337 (2016) 248-259.

[24] P. Ratnasamy, D. Srinivas, H. Knözinger, Adv. Catal. 48 (2004) 1-169.

[25] Z. Zhuo, L. Wang, X. Zhang, L. Wu, Y. Liu, M. He, J. Catal. 329 (2015) 107-118.

[26] S. Bordiga, C. Lamberti, F. Bonino, A. Travert, F. Thibault-Starzyk, Chem. Soc. Rev. 44 (2015) 7262-7341.

[27] B. Gil, Acidity of zeolites, in: J. Cejka, J. Peréz-Pariente, W.J. Roth (Eds.) Zeolites: From Model Materials to Industrial Catalysts Transworld Research Network, 2008, pp. 173-207.

[28] W.J. Roth, J. Cejka, R. Millini, E. Montanari, B. Gil, M. Kubu, Chem. Mater. 27 (2015) 4620-4629.

[29] B. Gil, W.J. Roth, W. Makowski, B. Marszalek, D. Majda, Z. Olejniczak, P. Michorczyk, Catal. Today 243 (2015) 39-45.

[30] B. Gil, G. Kosova, J. Cejka, Microporous Mesoporous Mater. 129 (2010) 256-266.

[31] D.P. Serrano, R.A. Garcia, M. Linares, B. Gil, Catal. Today 179 (2012) 91-101.

[32] M. Bevilacqua, G. Busca, Catal. Commun. 3 (2002) 497-502.

[33] B. Gil, K. Kalahurska, A. Kowalczyk, Appl. Catal. A 578 (2019) 63-69.

[34] B. Gil, W. Makowski, B. Marszalek, W.J. Roth, M. Kubu, J. Cejka, Z. Olejniczak, Dalton Trans. 43 (2014) 10501-10511.

[35] B. Gil, B. Marszalek, A. Micek-Ilnicka, Z. Olejniczak, Top. Catal. 53 (2010) 1340-1348.

[36] M. Taramasso, G. Perego, B. Notari, in: H. Robson (Ed.) Verified Syntheses of Zeolitic Materials, Elsevier, Amsterdam, 2001, pp. 207.

[37] S. Brunauer, P.H. Emmett, E. Teller, J. Am. Chem. Soc. 60 (1938) 309-319.

[38] B.C. Lippens, J.H. de Boer, J. Catal. 4 (1965) 319-323.

[39] B. Gil, K. Kałahurska, A. Kowalczyk, Appl. Catal. A 578 (2019) 63-69.

[40] J.W. Harris, M.J. Cordon, J.R. Di Iorio, J.C. Vega-Vila, F.H. Ribeiro, R. Gounder, J. Catal. 335 (2016) 141-154.

[41] F. Thibault-Starzyk, B. Gil, S. Aiello, T. Chevreau, J.-P. Gilson, Microporous Mesoporous Mater. 67 (2004) 107-112.

[42] A. Corma, V. Fornés, F. Rey, Zeolites 13 (1993) 56-59.

[43] Y. Zhou, S.A. Kadam, M. Shamzhy, J. Čejka, M. Opanasenko, ACS Catal. 9 (2019) 5136-5146.

[44] Q. Yue, J. Zhang, M. Shamzhy, M. Opanasenko, Microporous Mesoporous Mater. 280 (2019) 331-336.

[45] M. Pitínová-Štekrová, P. Eliášová, T. Weissenberger, M. Shamzhy, Z. Musilová, J. Čejka, Catal. Sci. Tech. 8 (2018) 4690-4701.

[46] M. Thommes, K.A. Cychosz, Adsorption 20 (2014) 233-250.

[47] A. Travert, A. Vimont, A. Sahibed-Dine, M. Daturi, J.-C. Lavalley, Appl. Catal. A 307 (2006) 98-107.

[48] A. Zecchina, G. Spoto, S. Bordiga, M. Padovan, G. Leofanti, G. Petrini, IR Spectra of CO Adsorbed at Low Temperature (77 K) On Titaniumsilicalite, H-ZSM5 and Silicalite, in: G. Öhlmann, H. Pfeifer, R. Fricke (Eds.) Stud. Surf. Sci. Catal., Elsevier, 1991, pp. 671-680.

[49] F. Bonino, A. Damin, S. Bordiga, C. Lamberti, A. Zecchina, Langmuir 19 (2003) 2155-2161.

[50] T. Armaroli, M. Bevilacqua, M. Trombetta, A.d.G. Alejandre, J. Ramirez, G. Busca, Appl. Catal. A 220 (2001) 181-190.

[51] T.K. Phung, G. Busca, Appl. Catal. A 504 (2015) 151-157.

[52] T. Armaroli, M. Trombetta, A.G. Alejandre, J.R. Solis, G. Busca, Phys. Chem. Chem. Phys. 2 (2000) 3341-3348.

[53] C.O. Arean, M.R. Delgado, P. Nachtigall, H.V. Thang, M. Rubes, R. Bulanek, P. Chlubna-Eliasova, Phys. Chem. Chem. Phys. 16 (2014) 10129-10141.

[54] H.V. Thang, J. Vaculik, J. Prech, M. Kubu, J. Cejka, P. Nachtigall, R. Bulanek, L. Grajciar, Microporous Mesoporous Mater. 282 (2019) 121-132.

[55] H.V. Thang, K. Frolich, M. Shamzhy, P. Eliášová, M. Rubeš, J. Čejka, R. Bulánek, P. Nachtigall, Phys. Chem. Chem. Phys. 18 (2016) 18063-18073.

[56] R. Bulanek, M. Kolarova, P. Chlubna, J. Cejka, Adsorption 19 (2013) 455-463.

[57] B. Wichterlová, Z. Tvarůžková, Z. Sobalík, P. Sarv, Microporous Mesoporous Mater. 24 (1998) 223-233.

Quantification of Lewis acid sites in 3D and 2D TS-1 zeolites: FTIR spectroscopic study

Mariya Shamzhy*,[1], Jan Přech[1,2], Jin Zhang[1], Valérie Ruaux[2], Hussein El-Siblani[2], Svetlana Mintova[2]

[1] *Department of Physical and Macromolecular Chemistry, Faculty of Science, Charles University, Hlavova 2030/8, 128 43 Prague 2, Czech Republic*

[2] *Normandie Université, ENSICAEN, UNICAEN, CNRS, Laboratoire Catalyse et Spectrochimie, 14000 Caen*

*Corresponding author:mariya.shamzhy@natur.cuni.cz

Keywords: TS-1, layered zeolites, acidity, FTIR, molar extinction coefficient

Figure S1. XRD patterns of 3D TS-1(a) (gray), 3D TS-1(b) (black), 2D TS-1 (red), TS-1-PISi (green), TS-1-PITi (blue)
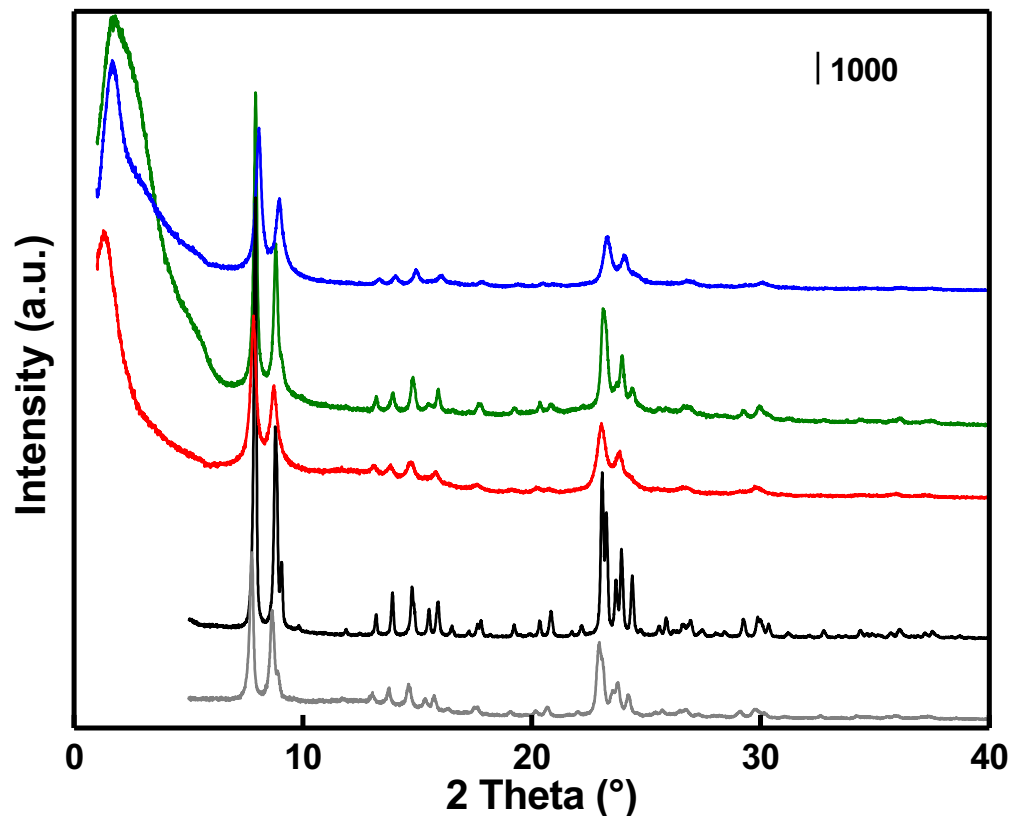
Figure S2. N_2 ad-/desorption isotherms of 3D TS-1(a) (gray), 3D TS-1(b) (black), 2D TS-1 (red), TS-1-PISi (green), TS-1-PITi (blue)
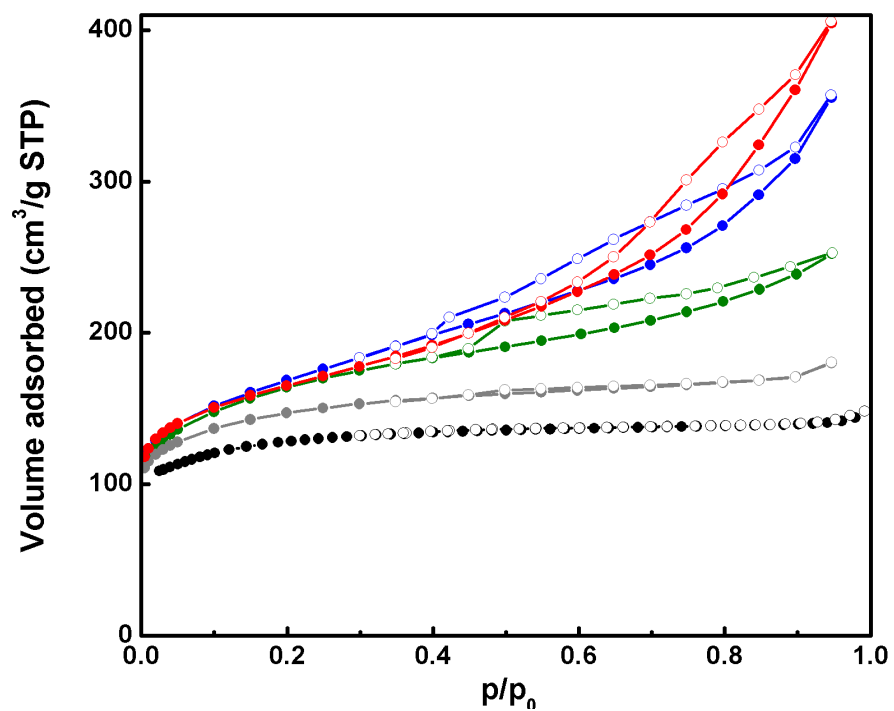
Figure S3. SEM images of 3D TS-1(a) (a), 3D TS-1(b) (b), 2D TS-1 (c), TS-1-PISi (d), TS-1-PITi (e)
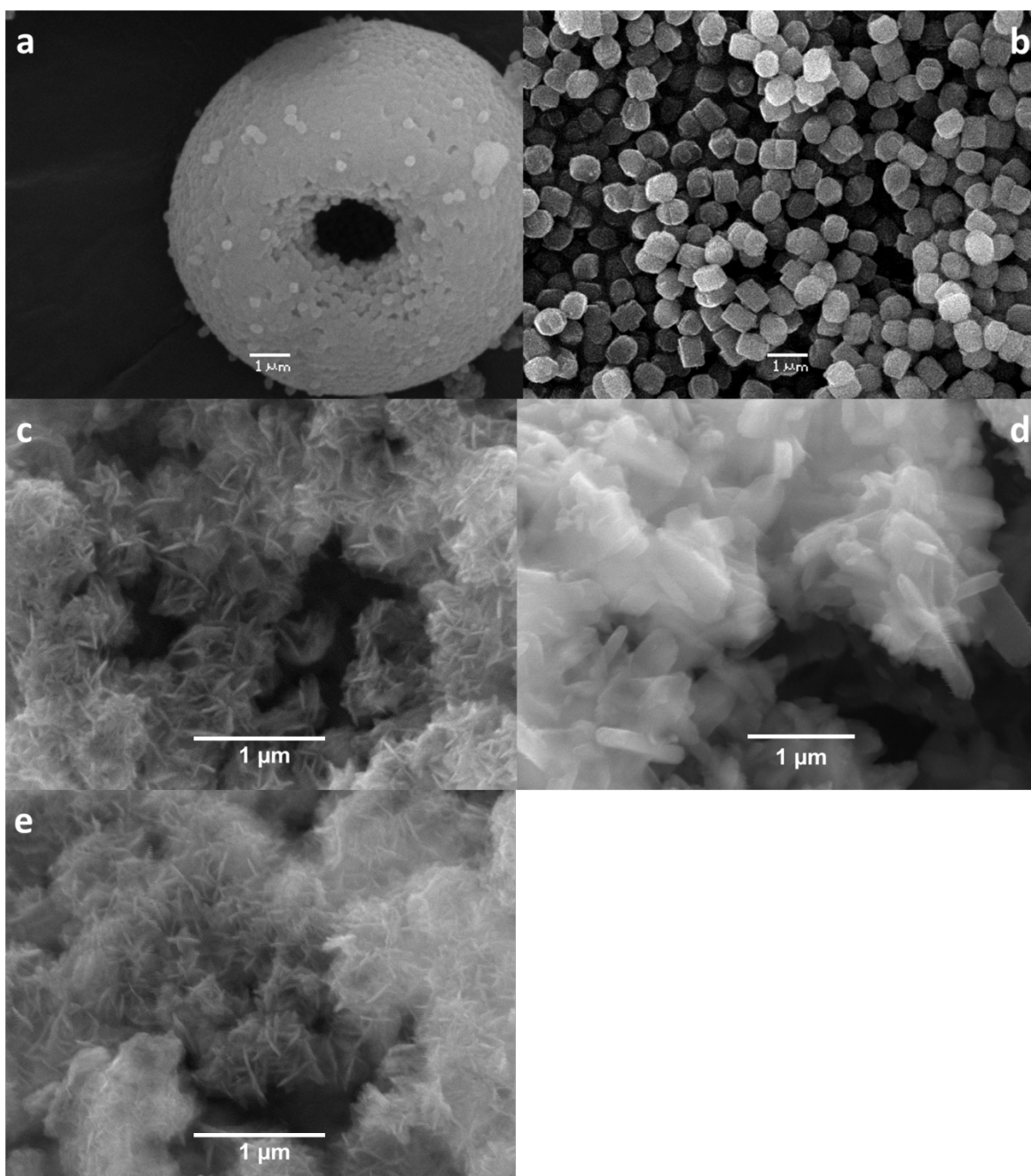
Figure S4. TPD-NH$_3$ curves for 3D TS-1(a) (grey), 3D TS-1(b) (black), TS-1-PITi (blue)